C S I R O   P U B L I S H I N G

Australian Journal of Physics

Volume 52, 1999

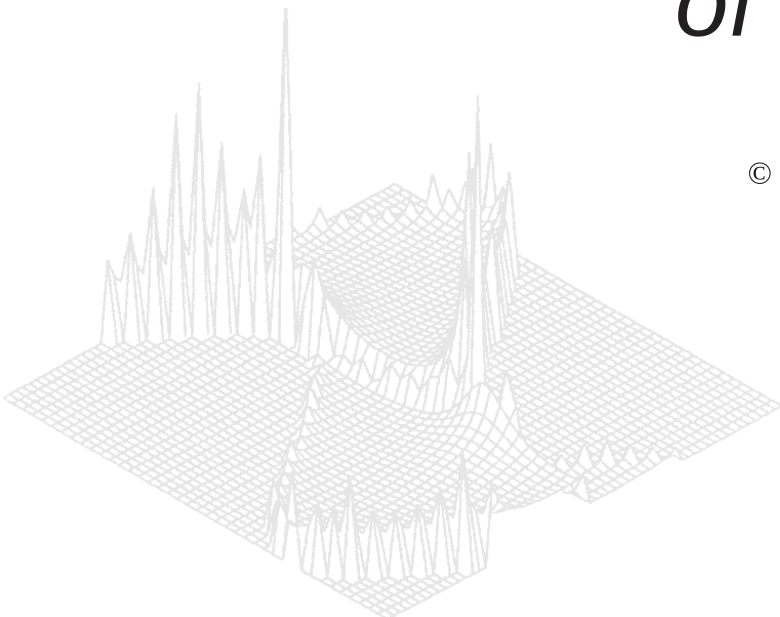

A journal for the publication of
original research in all branches of physics

www.publish.csiro.au/journals/ajp

All enquiries and manuscripts should be directed to
Australian Journal of Physics
CSIRO PUBLISHING
PO Box 1139 (150 Oxford St)
Collingwood
Vic. 3066
Australia
Telephone: 61 3 9662 7626
Facsimile: 61 3 9662 7611
Email: peter.robertson@publish.csiro.au

Published by **CSIRO** PUBLISHING
for CSIRO Australia and
the Australian Academy of Science

Aust. J. Phys., 1999, **52**, 859–85

Two-dimensional Scattering by a Potential without a Classical Analogue*

I. V. Ponomarev

School of Physics, University of New South Wales,
Sydney, NSW 2052, Australia.
Present address: Department of Physics, University of Utah,
Salt Lake City, UT 84112, USA.

Abstract

A two-dimensional scattering potential represents the quantum extension of a diffractive lattice: a Dirac delta function with a modulated permeability along the y-axis. This model does not have an explicit classical analogue and quantum effects such as tunneling and diffraction play an important role. An analytical solution for the one-harmonic case is found. For the general case of an arbitrary number of harmonics a simple criterion is derived for the range of parameters where quantum chaos is permitted (but does not necessarily occur). The statistical properties of the S-matrix for the given model have been investigated. The deviations from the usual predictions for irregular scattering in the random matrix theory (RMT) framework have been found and are discussed.

1. Introduction

Nowadays, the term 'quantum chaos' is commonly used for dynamical quantum systems that are chaotic in the classical limit. The aim of the present paper is to analyse one simple scattering model that has no explicit classical analogue and in which quantum effects such as tunneling and diffraction have the most important role even in the short wave limit. The classical description of chaotic scattering has been analysed quite thoroughly and the essential result is the following. The scattering is chaotic if there is a fractal set in phase space which is called the chaotic repeller. Its existence can be seen in the singularities of the deflection (or time delay) function (Manakov and Shchur 1983; Bleher *et al.* 1989), which connects the outgoing parameters after scattering with the input conditions. The complexity of the deflection function is directly related to the existence of an infinite number of orbits 'trapped' in the interaction region, which are responsible for the formation of the general structure for chaotic motion.

In the quantum description of such systems the S-matrix plays an important role. A knowledge of the chaotic repeller properties has been shown (Smilansky 1992; Gaspard and Rice 1989) to enable one to investigate the peculiarities of scattering resonances and the statistical properties of the S-matrix in the semiclassical limit. There is a hypothesis that the quantum behaviour of classically

* Refereed paper based on a contribution to the Eighth Gordon Godfrey Workshop on Condensed Matter Physics held at the University of New South Wales, Sydney, in November 1998.

 10.1071/PH98095 0004-9506/99/050859$10.00

chaotic systems displays universal features. The scattering matrix corresponding to such processes in the limit of small $\hbar$ fluctuates according to the prediction of the RMT (Porter 1965; Mehta 1990). Namely, the distribution of the square moduli of the S-matrix elements is Poissonian; the distribution of the nearest neighbour spacings between the eigenphases is a Wigner–Dyson one (i.e., there is a 'repulsion' at small spacings):

$$P(s) \propto s e^{-Bs^2} . \tag{1}$$

Moreover, whenever the S-matrix is dominated by resonances whose widths exceed their spacing, the energy dependence of the cross section $\sigma_{nm}(E)$ shows Ericson (1963) fluctuations with a Lorentzian auto-correlation function. The width of the Lorentzian gives the mean resonance width. Another important feature that characterises quantum chaotic scattering is the distribution of the poles of the S-matrix in the complex energy plane. It was shown that for some typical scattering problems poles are excluded from a strip: they cannot come closer to the real axis from below than a finite distance Γ_b.

Although classically chaotic scattering processes display random matrix properties of the eigenphases of S, the reverse is not always true (Blümel *et al.* 1992). Namely, the random matrix properties of an S-matrix for the quantum system do not necessarily mean that its classical counterpart is chaotic. A semiclassical approach, based on Poincarè scattering mapping (PSM) (Jung 1986), which is the classical analogue of the S-matrix, sheds more light on the problem. A classical system may be regular (that is, it supports only a countable set of trapped orbits) and so its deflection function will have a simple structure. In spite of this, the corresponding PSM may be regular, hyperbolic or display mixed dynamics. We can say that the degree of irregularity of the PSM serves as a more sensitive test for the transition to chaotic scattering in the classical domain. Moreover, it is the properties of the PSM that determine the chaotic behaviour of the corresponding S-matrix in the quantum domain.

As an example, let us recall the model (Smilansky 1992; Blümel *et al.* 1992) of an infinite array of identical non-overlapping disc potentials, equally spaced along the y-axis in a plane. If the scattering potentials are attractive and the deflection angle is sufficiently large then the classical scattering is chaotic and all statistical properties of the corresponding quantum S-matrix are in good agreement with the RMT predictions. The case of repulsive hard discs does not show classical chaotic scattering since there exists only one unstable trapped periodic orbit along the segment of the y-axis between neighbouring discs. Nevertheless, the PSM in this problem is hyperbolic. The nearest-neighbour distribution of the phases of the S-matrix is in very good agreement with the Wigner function. Other characteristics, such as the distribution of the normalised transition elements, show appreciable deviations from the predictions of the RMT for the canonical ensemble of unitary, symmetric matrices (CUE).

However, it is worth while pointing out that there are systems without explicit classical analogues. For such systems the quantum effects have the most important role even in a deep semiclassical region. The question about the possibility of chaotic phenomena and their connection with RMT predictions in such systems is still open. The dynamical model of resonance scattering on a 'diffractive lattice' with modulated permeability is proposed below as an attempt to clarify this question.

The two-dimensional scattering potential is represented by a Dirac delta function with modulated permeability along the y-axis (a potential barrier with varying potential strength in the y-direction). Our model partially resembles the above-mentioned example (Smilansky 1992) but, in contrast to it, there is no chaos in the high energy limit at all. Moreover, it is not possible to construct a corresponding PSM because in the classical limit some trajectories fall into the infinitely deep attractive regions of the potential (we suggest that the modulation function is able to change sign). Another distinctive feature of the model is that the permeability function can have a diverse behaviour: periodic, quasi-periodic or even chaotic. Accordingly, the complexity of the potential governs the features of the S-matrix. In this paper we briefly discuss the quasi-periodic modulation of the permeability and concentrate mostly on the periodic case.

Another advantage of the model is its relative simplicity. The analytical consideration allows one to reduce the solution of the model to a system of linear algebraic equations, which is very convenient for the numerical simulation. The one-harmonic case, when the modulation function is a simple cosine, admits even further analytical treatment.

The structure of the paper is the following: in Section 2 the model is described and the equations for the S-matrix are derived. The symmetry and other properties of the scattering operator are discussed. In Section 3 we carry out a detailed numerical investigation of the statistical properties of the S-matrix for the periodic potential with different degrees of complexity. We finally summarise and discuss our results in Section 4. The mathematical details of the calculations are outlined in the Appendices.

2. The Model

We study the problem of two-dimensional scattering of a particle on a potential with modulated diffractive lattice and a mirror*

$$U(x,y) = \begin{cases} \dfrac{\hbar^2}{\mu\alpha}\,\delta(x)g(y), & x \le d \\ \quad\infty\ , & x \ge d. \end{cases} \qquad (2)$$

Here $\delta(x)$ is the Dirac delta function and

$$g(y) = \sum_{m=-\infty}^{\infty} \beta_m \left(e^{iym\nu_g} + e^{iym\nu_f}\right)\,,$$

$$\beta_m \le 1, \quad \beta_{-m} = \beta_m^*\,, \qquad (3)$$

where α is the transparency of the barrier, while ν_g, ν_f and β_m are, respectively, the frequencies and amplitudes of the modulation. A sketch of the potential is presented in Fig. 1.

There are two situations for which chaos could possibly appear in the problem. The first one may occur when the frequencies are commensurable ($\nu_g/\nu_f = r/s$,

* We use the mirror in order to create the resonance structure in the region $0 \le x \le d$ and to halve the dimension of the S-matrix.

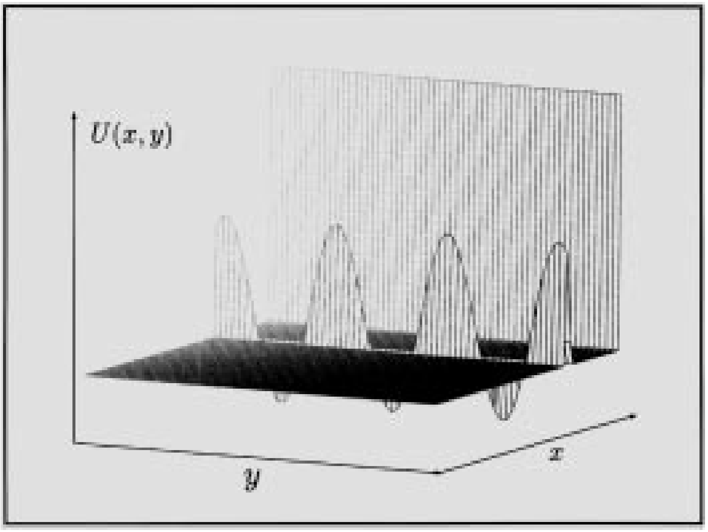

Fig. 1. Sketch of the 2D potential for the model.

where r, s are the mutual primes) and $\sum_{m=1}^{\infty} |\beta_m| > \frac{1}{2}$. The last condition means that the attraction regions appear in the potential [the function $g(y)$ can change sign]. The naive classical picture would correspond to the case when the particle is trapped by the lattice for a long time.

The second case is connected with the breakdown of quasi-momentum (which is the second integral of the motion in addition to the energy) when the frequencies of modulation are incommensurable. The $\hat{S}$-operator is the infinite matrix $S_{mn,rs}$ which is determined from the double-index system of linear equations. The numerical investigation of the system and the statistical properties of the S-matrix in this case demand another analytical approach and will be published elsewhere.

Hereafter we only consider the first situation in which the modulation function is periodic (with one fundamental frequency ν):

$$g(y) = g(y + 2\pi/\nu) = \frac{1}{\alpha} \sum_{m=-\infty}^{\infty} \beta_m e^{iym\nu} \,. \tag{4}$$

It is worth noting that the case of two commensurable frequencies (3) reduces to equation (4), because the function $g(y)$ is periodic with a smaller fundamental frequency:

$$\nu = \frac{\nu_g}{r} = \frac{\nu_f}{s}.$$

Moreover, the incommensurability can be treated as a limit of successive approximations of an irrational number by rational ones [for example with the help of continued fractions (Jones and Tron 1980)].

The scattering process is determined by the diffraction and tunneling and, therefore, the model does not have an immediate counterpart in classical mechanics.

To find the equations for the S-matrix elements we solve the integral equation

$$\Psi_{\vec{k}}(\vec{r}) = e^{ik_y y}\left(e^{ik_x x} - e^{-ik_x(x-2d)}\right) + \frac{2\mu}{\hbar^2}\int \mathcal{G}(\vec{r};\vec{r}')U(\vec{r}')\Psi_{\vec{k}}(\vec{r}')d\vec{r}'\,, \tag{5}$$

where

$$k^2 = k_x^2 + k_y^2, \qquad \vec{r} = (x, y) \quad \text{and} \quad \vec{k} = (k_x, k_y)\,. \tag{6}$$

This corresponds to the time-independent Schrödinger equation with boundary conditions at infinity as incident plane and outgoing cylindrical waves.

In equation (5) $\mathcal{G}(\vec{r};\vec{r}')$ is the Green's function for a free particle whose motion is confined by an impenetrable wall:

$$\begin{aligned}\left[\nabla_{\vec{r}}^2 + k^2\right]\mathcal{G}(\vec{r};\vec{r}') &= \delta(\vec{r}-\vec{r}'), \quad x, x' \le d\\ \mathcal{G}(\vec{r};\vec{r}') &= 0, \qquad\qquad x, x' \ge d\,.\end{aligned} \tag{7}$$

It is simple to show that

$$\begin{aligned}\mathcal{G}(\vec{r};\vec{r}') &\equiv \frac{1}{4i}G(x, x'; y-y')\\ &= \frac{1}{4i}[H_0^{(1)}(k\sqrt{(x-x')^2+(y-y')^2})\\ &- H_0^{(1)}(k\sqrt{(x+x'-2d)^2+(y-y')^2})]\,.\end{aligned} \tag{8}$$

Here $H_0^{(1)}(kr)$ is Hankel's function of first type and zeroth order. After a substitution of (2) and (8) into (5) we get

$$\begin{aligned}\Psi_{\vec{k}}(x, y) &= e^{ik_y y}\left(e^{ik_x x} - e^{-ik_x(x-2d)}\right)\\ &- \frac{i}{2}\int_{-\infty}^{\infty} G(x, 0; y-y')g(y')\Psi_{\vec{k}}(0, y')dy'\,.\end{aligned} \tag{9}$$

The right-hand side of (9) shows that to obtain the $\Psi_{\vec{k}}(x, y)$ one only needs to find $\Psi_{\vec{k}}(0, y)$:

$$\Psi_{\vec{k}}(0, y) = e^{ik_y y}\left(1 - e^{ik_x 2d}\right) - \frac{i}{2}\int_{-\infty}^{\infty} G(0, 0; t)g(t+y)\Psi_{\vec{k}}(0, t+y)dt\,. \tag{10}$$

The solution can be written in the form of Bloch waves:

$$\Psi_{\vec{k}}(0, y) = e^{iqy}\sum_{n=-\infty}^{\infty}\varphi_n e^{iyn\nu} = e^{iqy}\varphi(y)\,; \tag{11}$$

$$\varphi(y) = \varphi\left(y + \frac{2\pi}{\nu}\right),$$

with the quasi-momentum being fixed in the first zone:

$$-\frac{\nu}{2} \le q \le \frac{\nu}{2}\,. \tag{12}$$

From substitution of (4) and (11) into (10), it follows that the periodicity of $\varphi(y)$ results in the condition

$$k_{y_l} \equiv k_y = q + l\nu, \qquad l = 0, \pm 1, \pm 2, \cdots \tag{13}$$

For a particular q there is a finite discrete number of input directions with

$$|k_{y_l}| < k\,, \tag{14}$$

where l is restricted as follows:

$$-L_{\min} \equiv -\left[\frac{k+q}{\nu}\right] \le l \le \left[\frac{k-q}{\nu}\right] \equiv L_{\max} \tag{15}$$

and $[\cdots]$ means the greatest integer less than a real number.

In other words, the discrete translational symmetry implies the quantisation of the y component of the momentum. Introducing the notation

$$k_{x_m} = \sqrt{k^2 - k_{y_m}^2} \qquad \text{(arithmetic branch)}, \tag{16}$$

we obtain the following system of linear equations for the expansion coefficients $\varphi_m^l \equiv \varphi_m$:

$$\begin{gathered} \alpha\varphi_m^l + i\frac{(1-e^{2ik_{x_m}d})}{k_{x_m}} \sum_{n=-\infty}^{\infty} \beta_n \varphi_{m-n}^l = \alpha(1-e^{2ik_{x_l}d})\delta_{ml}, \\ -\infty < m < \infty. \end{gathered} \tag{17}$$

Here the upper index 'l' enumerates the given incident direction $k_y^{(\mathrm{in})} = k_{y_l}$ and obeys the requirements (15).

If we substitute the coefficients φ_m^l, obtained from the solution of (17) into (9), we get the complete wave function:

$$\begin{aligned} \Psi_{k,q}^l(x,y) = e^{ik_{x_l}d} \sum_{m=-\infty}^{\infty} & e^{ik_{y_m}y}[\delta_{ml}e^{k_{x_l}(x-d)} \\ & - e^{-ik_{x_m}(x-d)}e^{-ik_{x_m}d}(\delta_{ml}-\varphi_m^l)e^{-ik_{x_l}d}]\,. \end{aligned} \tag{18}$$

The only values of $k_y^{(\text{out})}$ for the scattering waves are those which differ from the incoming values $k_y^{(\text{in})}$ by integer multiples of ν. In the asymptotic limit $x \longrightarrow -\infty$ only a finite number of terms in the series survive with $|k_{y_m}| < k$, since the other ones damp out exponentially along the x-coordinate. Taking into consideration the probability flux normalisation, the S-matrix elements can be written in the following manner:

$$\hat{S}(k_y; k'_y) = \hat{S}(q, m; q', l) = \delta(q - q') S_{ml}(q) \,, \tag{19}$$

where

$$S_{ml}(q) \equiv S_{ml} = e^{-ik_{x_m} d} \left[\delta_{ml} - \sqrt{\frac{k_{x_m}}{k_{x_l}}} \varphi^l_m \right] e^{-ik_{x_l} d} \tag{20}$$

or

$$\hat{S} = \hat{S}^{\text{pot}} \hat{S}^{\text{res}} \hat{S}^{\text{pot}}, \qquad S^{\text{res}}_{ml} = \delta_{ml} - \sqrt{\frac{k_{x_m}}{k_{x_l}}} \varphi^l_m \,. \tag{21}$$

The integers m and l are restricted by the condition (15). The size of the S-matrix is equal to $N_{\text{op}} = L_{\min} + 1 + L_{\max}$.

Here $\hat{S}^{\text{pot}}$ is a diagonal matrix which represents the trivial phase shifts between the lattice and the mirror. The matrix $\hat{S}^{\text{res}}$ contains all the information about the S-matrix poles.

In the two opposite limits, when α goes to ∞ or zero, the S-matrix is diagonal and has a simple behaviour:

$$\begin{aligned} S_{ml} &\longrightarrow \delta_{ml} && \text{at } \alpha \longrightarrow \infty, \\ S_{ml} &\longrightarrow \delta_{ml} e^{-2ik_{x_l} d} && \text{at } \alpha \longrightarrow 0 \,. \end{aligned} \tag{22}$$

The magnitude $\sigma_{ml} = |\delta_{ml} - S_{ml}|^2$ is the differential cross section which corresponds to the probability of scattering from the lth incoming direction to the mth outcoming one. It is possible to say that each direction k_{y_n} plays the role of a scattering channel. The allowed values of k_y (for a given q and k) correspond to the open channels and the directions which do not satisfy (14) correspond to closed ones. As the particle energy increases, new open channels appear. The corresponding threshold energies are

$$k^2 = k^2_{ym} \,. \tag{23}$$

Because of flux conservation $\hat{S}$ is unitary:

$$\hat{S}\hat{S}^\dagger = \hat{S}^\dagger \hat{S} = \hat{I} \,. \tag{24}$$

From time-reversal symmetry it is obvious that (Landau and Lifshitz 1965)

$$\hat{S}(k_y; k'_y) = \hat{S}(-k'_y; -k_y) \Rightarrow S_{ml}(q) = S_{-l-m}(-q) \,. \tag{25}$$

It should be noted that for a fixed quasi-momentum the S-matrix is not symmetric. However, if $g(y)$ is an even or odd function [i.e. the function $g(y)$ has a symmetry axis], then

$$\hat{S}(k_y; k'_y) = \hat{S}(-k_y; -k'_y) \Rightarrow S_{ml}(q) = S_{-m-l}(-q) \tag{26}$$

and the conditions (25) and (26) together imply that the S-matrix is symmetric.

It will be instructive to look at the case $g(y) = 1$, which corresponds to the one-dimensional problem. Then the S-matrix is diagonal:

$$\hat{S} = \delta(k_y - k'_y) S(k_x) = \delta(q - q')\delta_{lm} S(k_{xl}),$$

where

$$S(k_x) = \frac{\alpha k_x - i(1 - e^{-2ik_x d})}{\alpha k_x + i(1 - e^{2ik_x d})} = e^{-2ik_x d} \prod_n \frac{(k_x - k_{xn}^*)(k_x + k_{xn})}{(k_x - k_{xn})(k_x + k_{xn}^*)}, \tag{27}$$

and $(S^{\text{pot}})^2 = e^{-2ik_x d}$ gives the retardation in phase corresponding to the path difference $2d$ between the wave reflected from the mirror and wave reflected from the δ-functional barrier. When $\alpha = 0$, we have bound states in the region $0 \le x \le d$, with $k_{xn} = n\pi/d$. When $\alpha k \ll 1$, there is a small probability of 'leaking' through the barrier and we observe resonances. The S-matrix has poles in the complex $z = k_x d$ plane. Their values are found from the solution of the transcendental equation

$$1 - e^{2ik_x d} = i\alpha k\,, \tag{28}$$

and we obtain poles at

$$k_{xn} d \approx n\pi \frac{1}{1 + \alpha/2d} - i\left(\frac{n\pi\alpha}{2d}\right)^2, \qquad \alpha k \ll 1\,. \tag{29}$$

It is worth noting that the δ-potential has a special property; namely, in the limit $\alpha \to 0$ the number of and the width of the resonances do not depend on whether the potential is attractive or repulsive.

In the case when only one harmonic is present [i.e. $g(y) = \beta_0 + 2\beta\cos(\nu y)$] the analytical treatment may be continued further.

The division of each equation in (17) by $i(1 - e^{2ik_{x_m} d}/k_{x_m})$ gives a tridiagonal system of linear equations as in Appendix A. Its solution may be expressed in terms of the continued fractions $f_n^{(\pm)}$ (see equations A13 and A14)

$$\varphi_{ll} = \frac{\lambda_l}{a_l - \beta\left[f_{l-1}^{(-)} + f_{l+1}^{(+)}\right]},$$

$$\varphi_{nl} = (-1)^{|l-n|}\varphi_{ll} \times \begin{cases} \prod_{j=n}^{l-1} f_j^{(-)}, & n < l \\ \prod_{j=l+1}^{n} f_j^{(+)}, & n > l \end{cases}. \tag{30}$$

Here we have

$$f_n^{(\pm)} = \frac{1}{a_n/\beta - f_{n\pm1}^{(\pm)}} \tag{31}$$

and

$$a_m = \frac{\beta_0\left(1 - e^{2ik_{x_m}d}\right) - i\alpha k_{x_m}}{1 - e^{2ik_{x_m}d}}, \qquad \lambda_m = -i\alpha k_{x_m}\,. \tag{32}$$

Thus, if we can find the continued fraction's remainders $f_{\pm N}^{(\pm)}$, starting from some particular $N > L_{\max}, L_{\min}$ we can construct the whole S-matrix by using (30), (31) and (20). These remainders are calculated in Appendix B. The question about convergence (i.e. where the continued fraction can be interrupted in order to get a solution with a given accuracy) is discussed there as well.*

The remainders at $n \gg k/\nu$ turn out to to be energy-independent and equal to

$$f_{\pm n}^{(\pm)} = \frac{\mathbf{J}_{\beta_0/\tilde{\alpha}\pm\tilde{q}+n}\left(2\beta/\tilde{a}\right)}{\mathbf{J}_{\beta_0/\tilde{\alpha}\pm\tilde{q}+n-1}\left(2\beta/\tilde{a}\right)}, \tag{33}$$

where $\mathbf{J}_x(z)$ is a Bessel function. In numerical calculations the continued fractions may be interrupted at the jth iteration, where

$$j > \frac{2\beta - \beta_0}{\alpha\nu}.$$

In the many-harmonic case another method (see Appendix C), similar to that in Blümel and Smilansky (1989), is more convenient for computing φ_{ml}.

For the sake of completeness we also present without derivation the equations for the $\hat{S}$ operator in the general case of incommensurable modulation frequencies:

$$g(y) = \sum_{n=-\infty}^{\infty}\left[g_n e^{in\nu_g y} + f_n e^{in\nu_f y}\right]\,. \tag{34}$$

The solution of (10) in this case is

$$\Psi_{\vec{k}}(0,y) = e^{ik_y^{\rm in}y}\sum_{m,n=-\infty}^{\infty}\varphi_{mn}e^{i(\nu_g m+\nu_f n)y} = e^{ik_y^{\rm in}y}\varphi(y)\,, \tag{35}$$

where $\varphi(y)$ is a quasi-periodic function, and k_y^{in} is the y-component of the incident wave vector. The coefficients φ_{mn} are determined from the following system of two-index linear equations:

$$\varphi_{mn}^{00} + \frac{i(1-e^{2ik_{x_{mn}}d})}{k_{x_{mn}}}\sum_{l=-\infty}^{\infty}\left[g_l\varphi_{m-ln}^{00} + f_l\varphi_{mn-l}^{00}\right] = \delta_{m0}\delta_{n0}\left(1 - e^{2ik_{x_{00}}d}\right)\,. \tag{36}$$

* This is also related to the point of truncation of the infinite dimensional matrix (17) in numerical simulations.

Here we have

$$k_{y_{mn}} = k_y^{\text{in}} + \nu_g m + \nu_f n, \qquad -\infty < n, m < \infty$$
$$k_{x_{mn}} = \sqrt{k^2 - k_{y_{mn}}^2}\,, \tag{37}$$

and the upper indexes designate the incident direction $k_{y_{00}} \equiv k_y^{\text{in}}$. There is an infinite (but countable) number of other input channels, which may be represented in the form of

$$k_{y_{rs}} = k_y^{\text{in}} + (r\nu_g + s\nu_f); \quad r, s = 0, \pm 1, \pm 2, \ldots$$

and a corresponding system of linear equations for φ_{mn}^{rs} may be written. The $\hat{S}$-matrix in this situation is

$$\mathrm{S}_{mn,rs} \;=\; \sqrt{\frac{k_{x_{mn}}}{k_{x_{rs}}}}\,(\delta_{mr}\delta_{ns} - \varphi_{mn}^{rs})\,. \tag{38}$$

It should be pointed out that the S-matrix is infinite dimensional since one may always find values of m and n that are of different sign and are as large as desired that satisfy the condition

$$|m|\nu_g - |n|\nu_f < k.$$

If $\nu_g = \nu_f = \nu$ and $g_l = f_l = \beta_l/2$, then the uniqueness of the solution implies that there is a 'sum rule':

$$\Psi_{\vec{k}}(0, y) = e^{iqy} \sum_{m=-\infty}^{\infty} \phi_m^l e^{i\nu m y} \equiv e^{ik_y^{in} y} \sum_{m,n=-\infty}^{\infty} \varphi_{mn}^{rs} e^{i\nu(m+n)y} \Rightarrow$$

$$\phi_m^l = \sum_{j=-\infty}^{\infty} \varphi_{jn-(r+s+j)}^{rs}\,. \tag{39}$$

Here we took into account $k_y^{\text{in}} = q + (r+s)\nu$.

3. Chaotic Properties of the S-Matrix

The first important conclusion follows immediately from equation (22). Due to a simple diagonal form for the two limiting cases for the S-matrix, it is obvious that chaos is only possible for values of α lying between certain lower and upper limits. When α tends to infinity, the potential is very weak and so the incoming particle is unaffected: $S_{ml} \longrightarrow \delta_{ml}$. All eigenphases are nearly degenerate (they are close to unity). The imaginary parts of the S-matrix poles are fairly large. The single resonance width is much larger than the mean distance between resonances and so the cross section is smooth.

In the other limit when the potential is strong ($\alpha \longrightarrow 0$), the S-matrix is diagonal again: $S_{ml} \longrightarrow \delta_{ml} e^{-2ik_{x_l}d}$. The distribution of nearest neighbour spacings between eigenphases is close to Poissonian. The resonance width is much smaller than the mean resonance spacing and the set of singularities of the cross section has a zero measure. A similar picture also appears when we fix α and the energy of the incoming particle tends to zero or infinity. It is worth pointing out that the same feature is inherent to the quasi-periodic modulation function (see equation 36).

Thus, we can only expect the possible appearance of chaos in the restricted range of the parameters where

$$\bar{\Gamma}/\overline{D} \sim 1\,. \tag{40}$$

Here $\bar{\Gamma}$ and $\overline{D}$ are the mean width of and the distance between resonances. This is exactly the region where the Ericson fluctuations are the most prominent!

Let us estimate the criterion (40) for our model. For the estimation of $\overline{D} \approx 1/\rho(k)$ we note that the coupling constant α does not influence the number of resonances (29) and in the limit $\alpha k \ll 1$ the position of the peaks is close to

$$k^2 = (n\pi/d)^2 + (l\nu)^2, \qquad l, n \text{ are integers.} \tag{41}$$

If we recall that the eigenvalues of a two-dimensional rectangular box with sides of length d and π/ν have the same spectrum, we immediately obtain from the Weil formula

$$N(k) \sim \frac{d\pi}{\nu 4\pi} k^2 \Rightarrow \bar{D}(k) \sim 2d\nu/k\,. \tag{42}$$

On the other hand, the resonance width is determined by the mean permeability α of the potential and can be roughly estimated from (29) also:

$$\bar{\Gamma}(k) \sim \left(\frac{\alpha k}{2d}\right)^2 . \tag{43}$$

Consequently, we have

$$\bar{\Gamma}/\overline{D} \sim \frac{\alpha^2 k^3}{d 8\nu} = \frac{(\alpha\nu)^2}{d} \left(\frac{N_{\rm op}}{4}\right)^3 . \tag{44}$$

Here $N_{\rm op} \sim 2k/\nu$ is the size of the S-matrix (the number of open channels).

In the numerical computations we took $N_{\rm op} \sim 50$, $\nu = 4$ and $d = 1$. For these values $\alpha \sim 5 \times 10^{-3}$ is required for the possible appearance of chaos and this is in correspondence with the behaviour of the cross section (see Fig. 2).

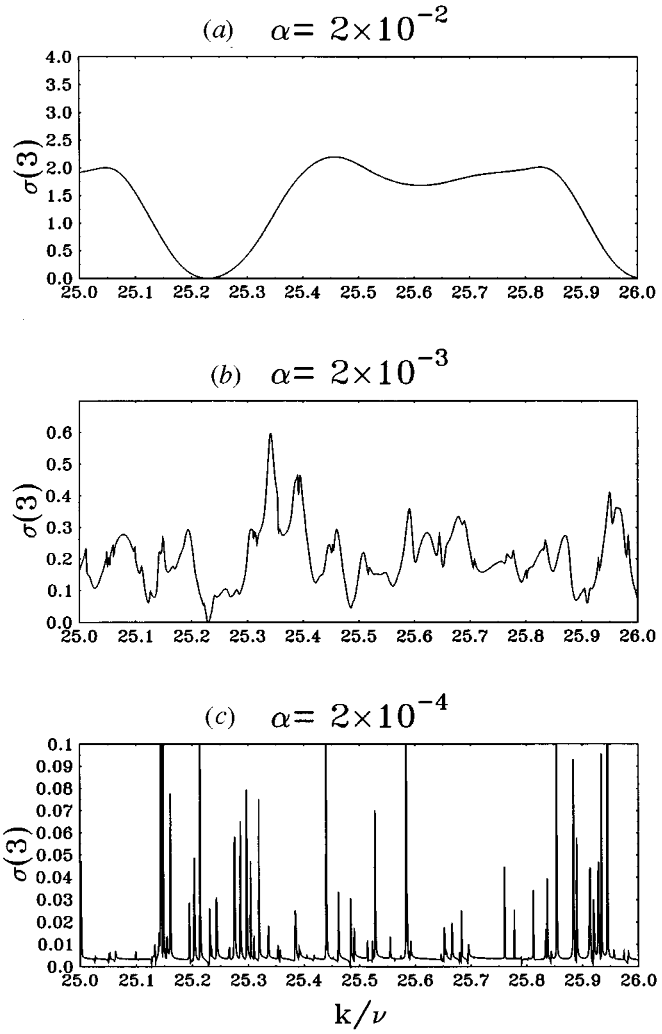

Fig. 2. Total cross section $\sigma(n) = \sum_m \sigma_{mn}$ for different transparencies α, with $g(y) = 0{\cdot}1{+}\cos(\nu y)$, $q = 0{\cdot}21$ and $\nu = 4$.

Fig. 3 shows the autocorrelation function which corresponds to Figs 2*b* and 2*c*. In the region of Ericson fluctuations the correlation length is equal to the mean resonance width estimated in (44).

It is worth noting that the presence of the tunneling mechanism results in the energy dependence of the quantum escape time and the absence of a constant gap between the real axis and the S-matrix poles in the complex energy plane (Csordás and Šeba 1993). A similar behaviour for the S-matrix is likely to occur for any system whose dynamics is determined by quantum tunneling.

Let us now investigate the influence of the modulation function complexity on the quantum scattering data. By 'complexity' we mean the number of terms (harmonics) in the expansion of $g(y)$ as a Fourier series.

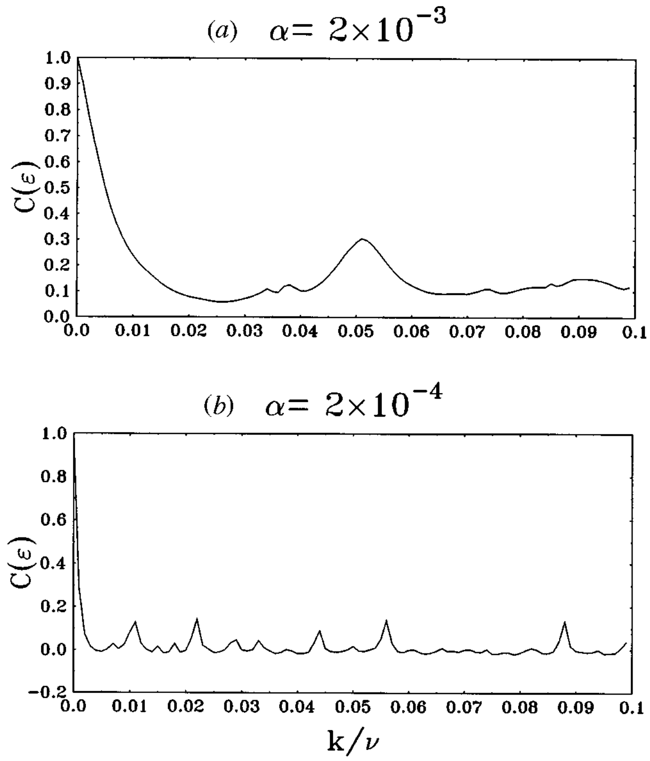

Fig. 3. Autocorrelation function $C(\varepsilon)$ for the total cross section $\sigma(3)$ (see Figs 2*b* and 2*c*).

Four forms of the periodic potential have been investigated ($T = 2\pi$):

$$
\begin{aligned}
&\text{I. } g(y) = \beta_0 + 2\beta_1 \cos(\nu y) \\
&\text{II. } g(y) = \cos(\nu y) + \sin(2\nu y + \phi_0) \\
&\text{III. } g(y) = \begin{cases} -1, |y| \le \pi/2 \\ \ \ 0, \text{ otherwise} \end{cases} \qquad \text{`rectangle'} \\
&\text{IV. } g(y) = \begin{cases} -1, & |y| \le \pi/3 \\ \ \ 1, & \pi/2 \le y \le 5\pi/6 \\ \ \ 0, & \text{otherwise} \end{cases} \qquad \text{`asymmetric rectangle'.}
\end{aligned}
\tag{45}
$$

The first and third forms of the potential give a symmetric S-matrix, while the third and fourth ones have many harmonics. We fix the value $q/\nu = 0{\cdot}21$ (if $q = 0$ then there is an additional symmetry $S_{ml} = S_{-m-l}$). The continued fractions technique allows us to investigate the S-matrix for the first potential up to $\alpha = 10^{-8}$. The other three forms of the potential were investigated numerically up to a value $\alpha = 2 \times 10^{-4}$.

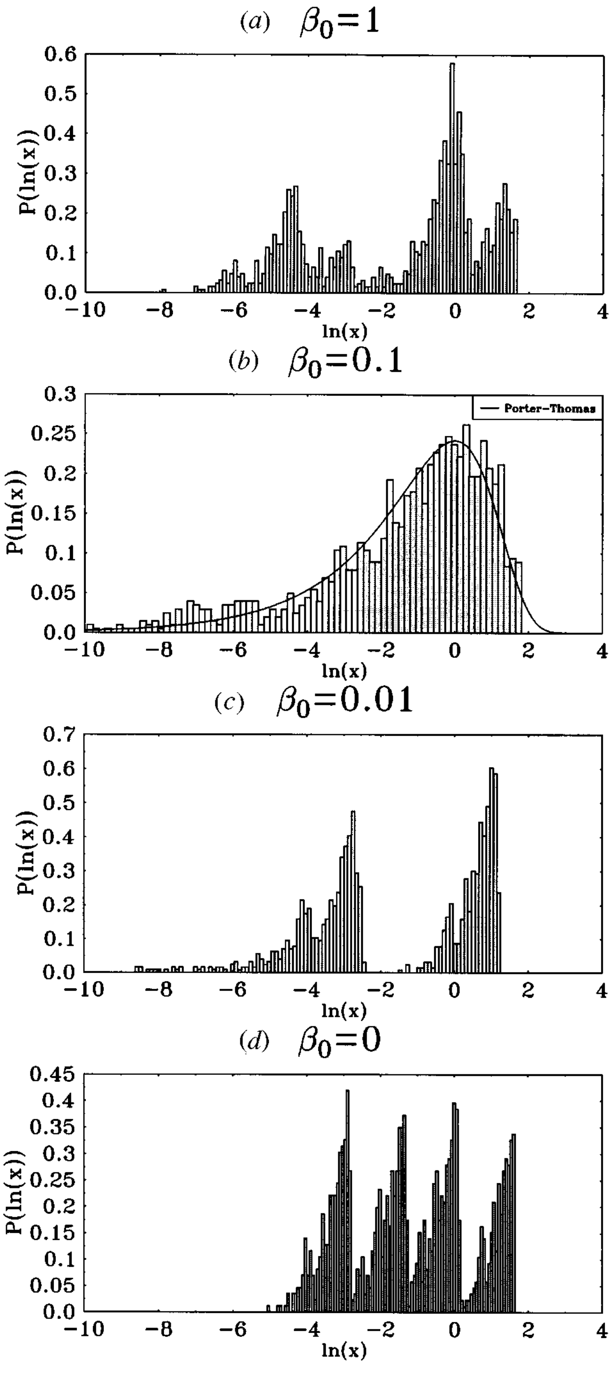

Fig. 4. Distribution of the square moduli of the T-matrix elements for $g(y) = \beta_0 + \cos(\nu y)$, $\alpha = 2 \times 10^{-5}$ and $gx = |T_{nm}|^2/\langle|T_{nm}|^2\rangle$.

Our first comparison between statistical properties of the S-matrix in the model and the RMT concerns the distribution of the normalised transition strength

$$x = |T_{ml}|^2 / \langle |T_{ml}|^2 \rangle \,, \tag{46}$$

where $\hat{T} = i(\hat{S} - \hat{I})$.

The RMT predicts that non-diagonal x will have a Poissonian distribution (Pereyra and Mello 1983). In our system, for all types of modulation function, this distribution shows appreciable deviations from the COE and CUE predictions.

The strong dependence of the moduli of the T-matrix elements on the coupling constant is noteworthy. At $\alpha \gtrsim 10^{-2}$ the T-matrix has a band structure with the strength of the elements decreasing smoothly from the main diagonal. When α is smaller, all the matrix elements have the same order of magnitude.

Fig. 4 shows the distribution $P(\ln(x))$ for $g(y) = \beta_0 + 2\beta_1 \cos(\nu y)$. As can be seen, the character of the distribution shows specific regularities which basically depend on the ratio between the zeroth and first harmonics strength β_0/β_1. They can be understood if we consider the system of equations on the T-matrix elements:

$$\left[\frac{i\alpha\sqrt{k_{x_m}}}{1 - e^{2ik_{x_m}d}} - \frac{\beta_0}{\sqrt{k_{x_m}}} \right] T_{m\ l} - \frac{\beta}{\sqrt{k_{x_{m-1}}}} T_{m-1\ l} - \frac{\beta}{\sqrt{k_{x_{m+1}}}} T_{m+1\ l} = \alpha\sqrt{k_{x_l}}\delta_{ml} . \tag{47}$$

In the limit of small α we look for a solution in the form of a power series in this parameter:

$$T_{ml} = \alpha T_{ml}^{(1)} + \alpha^2 T_{ml}^{(2)} + \ldots \tag{48}$$

Then we get

$$\frac{\beta_0}{\sqrt{k_{x_m}}} T_{m\ l}^{(1)} + \frac{\beta}{\sqrt{k_{x_{m-1}}}} T_{m-1\ l}^{(1)} + \frac{\beta}{\sqrt{k_{x_{m+1}}}} T_{m+1\ l}^{(1)} = -\sqrt{k_{x_l}}\delta_{ml} \,. \tag{49}$$

If β_0 equals zero (Fig. 4c) then the system (49) decouples into two independent subsystems with solutions

$$\begin{aligned} T_{2n+l\ l}^{(1)} &= 0, \\ T_{2n+1+l\ l}^{(1)} &= (-1)^{n+1} \left[\sqrt{k_{x_l} k_{x_{2n+1}}} + \sqrt{\frac{k_{x_{2n+1}}}{k_{x_{l+1}}}} T_{l+1\ l}^{(1)} \right] . \end{aligned} \tag{50}$$

More rigorous consideration shows that in this case there are four groups of matrix elements with values

$$T_{l+1\ l} \sim \alpha, \;\; T_{2n+l+1\ l} \sim \alpha k, \;\; T_{2n+l\ l} \sim \;\; T_{2n-1\ l} f_{2n} \,, \tag{51}$$

where f_{2n} is the continued fraction (31). A similar analysis shows that if β_0 is not equal to zero, but still small (see Fig. 4c and Fig. 7a), then there are two groups of matrix elements with relative strength $T_{m\ l}/T_{m+1\ l} \sim \beta_0/\beta$.

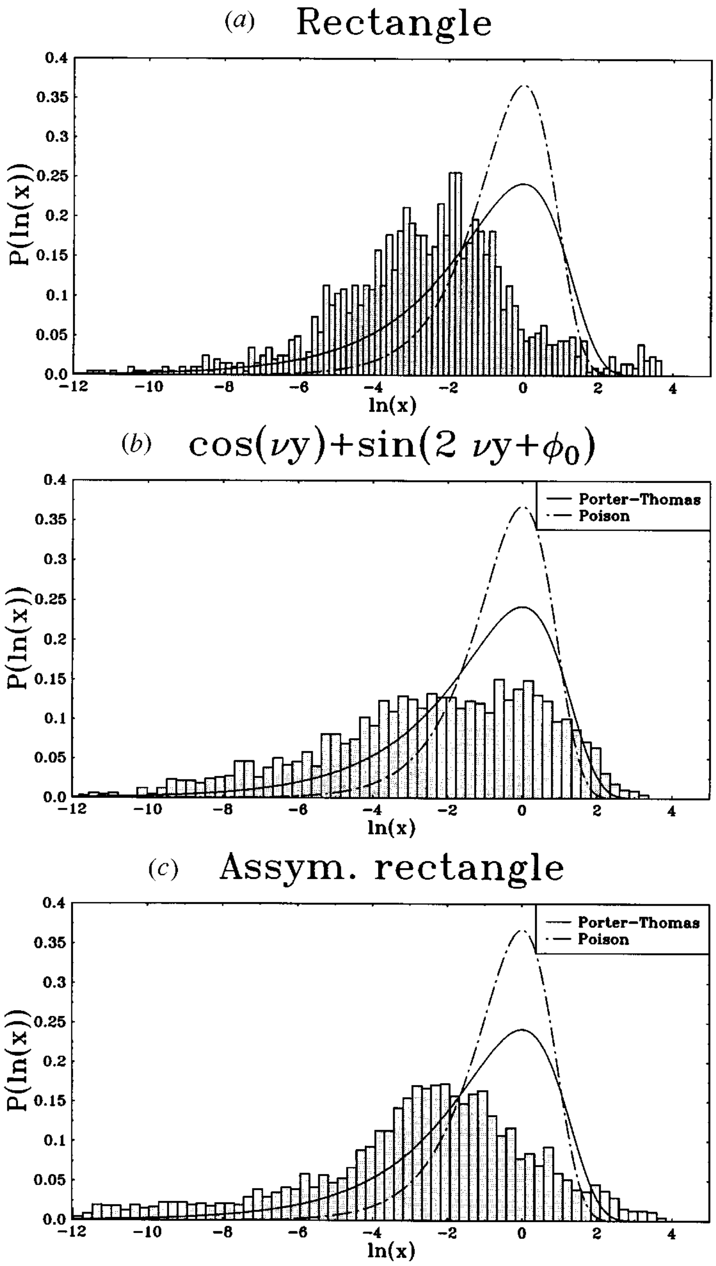

Fig. 5. Distribution of the square moduli of the T-matrix elements for different forms of the modulation function $g(y)$, with $x = |T_{nm}|^2/\langle|T_{nm}|^2\rangle$ and $\alpha = 2 \times 10^{-3}$.

However, over a wide range of β_0, for small enough permeability, the distribution is close to being a Porter–Thomas one as in Csordás and Šeba (1993). This distribution can be obtained analytically in the same manner as in Pereyra and Mello (1983), if we assume that the S-matrix elements have random moduli but correlated phases.

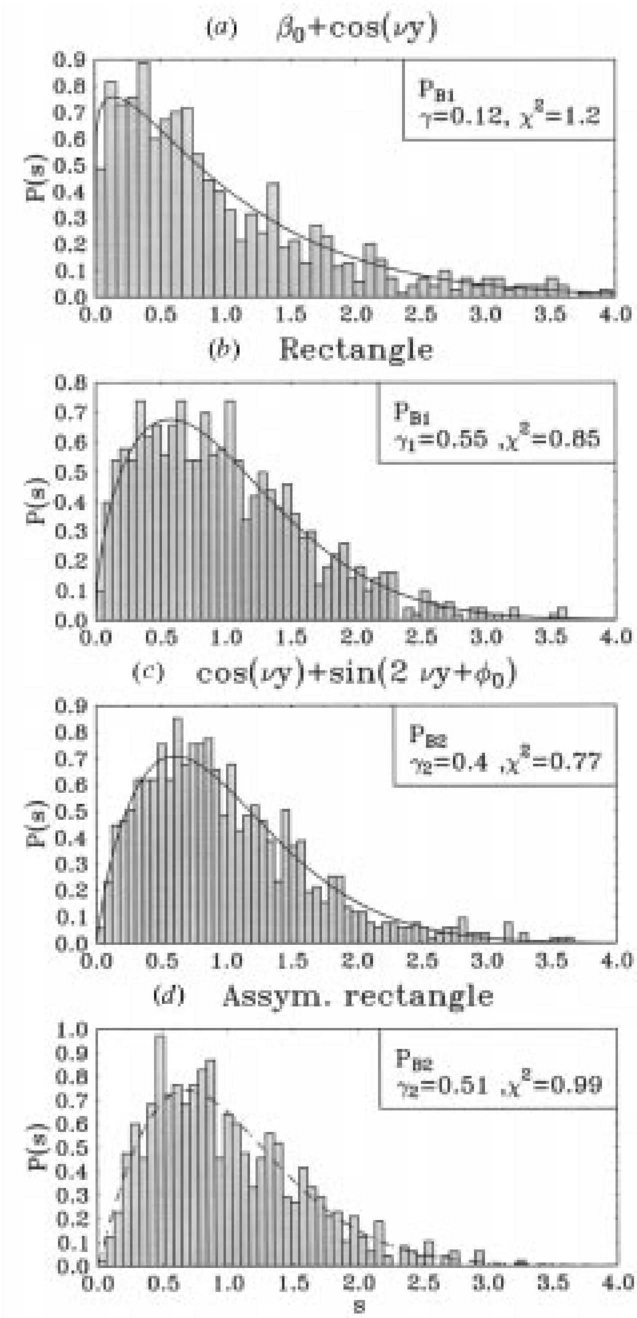

Fig. 6. Nearest neighbour spacing distribution of the S-matrix eigenphases. The parameter s is the spacing in units of the mean spacing $2\pi/N_{op}$. Part (a) corresponds Fig. 4b and parts (b)–(d) correspond to Fig. 5.

Finally, if we put $\beta_0 > 1$, then it will correspond to the renormalised function $\tilde{g}(y) = \beta_0 \left[1 + 2\tilde{\beta}\cos(\nu y)\right]$ with $\tilde{\beta} < 1$, and the T-matrix has a band structure in which the elements rapidly decrease away from the diagonal (see equation A15).

Fig. 5 shows $P(\ln(x))$ for the other potentials. The essential deflection from the RMT predictions can be observed again.

Another, less sensitive test is the distribution of the nearest neighbour spacings between the S-matrix eigenphases. For Dyson circular ensembles (COE and CUE) this distribution is described by the Wigner surmise:

$$P(s) = As^{\gamma}e^{-Bs^2} \qquad (\gamma = 1 \text{ or } 2)\,. \tag{52}$$

To get sufficient eigenphases statistics we vary the wave number over a small interval that, however, is much larger than the width of the autocorrelation function and therefore the S-matrices can be regarded as mutually independent.

It was found that the one-harmonic potential [(I) in equation (45) is regular—see Fig. 6*a*]. Nevertheless, a small repulsion was observed when the corresponding distribution of square moduli of the T-matrix elements is close to the Porter–Thomas one. It is worth noting that it is in this range of parameters where the Ericson fluctuations occur.

Increasing the complexity of the potential results in an enhancement of the repulsion (see Figs 6*b*, 6*c* and 6*d*). The distribution has intermediate statistics, which is to say that our model possesses weak chaotic properties only.

For a more quantitative measurement of the degree of repulsion we investigated the data by fitting them with two types of Brody-like distribution:

$$\begin{aligned} P_{B1}(s) &= As^{\gamma}e^{-bs^{1+\gamma}}, \\ &A = (1+\gamma)b, \qquad b = \left[\Gamma\left(\frac{2+\gamma}{1+\gamma}\right)\right]^{1+\gamma}, \end{aligned} \tag{53}$$

$$\begin{aligned} P_{B2}(s) &= As^{2\gamma}e^{-bs^{1+\gamma}}, \\ &A = (1+\gamma)b^2, \qquad b = \left[\Gamma\left(\frac{2\gamma+1}{\gamma+1}\right)\right]^{-(1+\gamma)}. \end{aligned} \tag{54}$$

The parameter γ was found by using the χ^2 approach:

$$\chi^2 = \frac{1}{n-2}\sum_{l=1}^{n}\frac{(O_l - E_l)^2}{E_l}\,, \tag{55}$$

where O_l and E_l are the expected and experimental values for the lth bin of the distribution. As a result, it was found that $P(s)$ for a symmetric S-matrix is well described by the Brody distribution P_{B1}. For an asymmetric one, a better fitting was by P_{B2}, which corresponds to intermediate statistics between Poisson and CUE predictions.

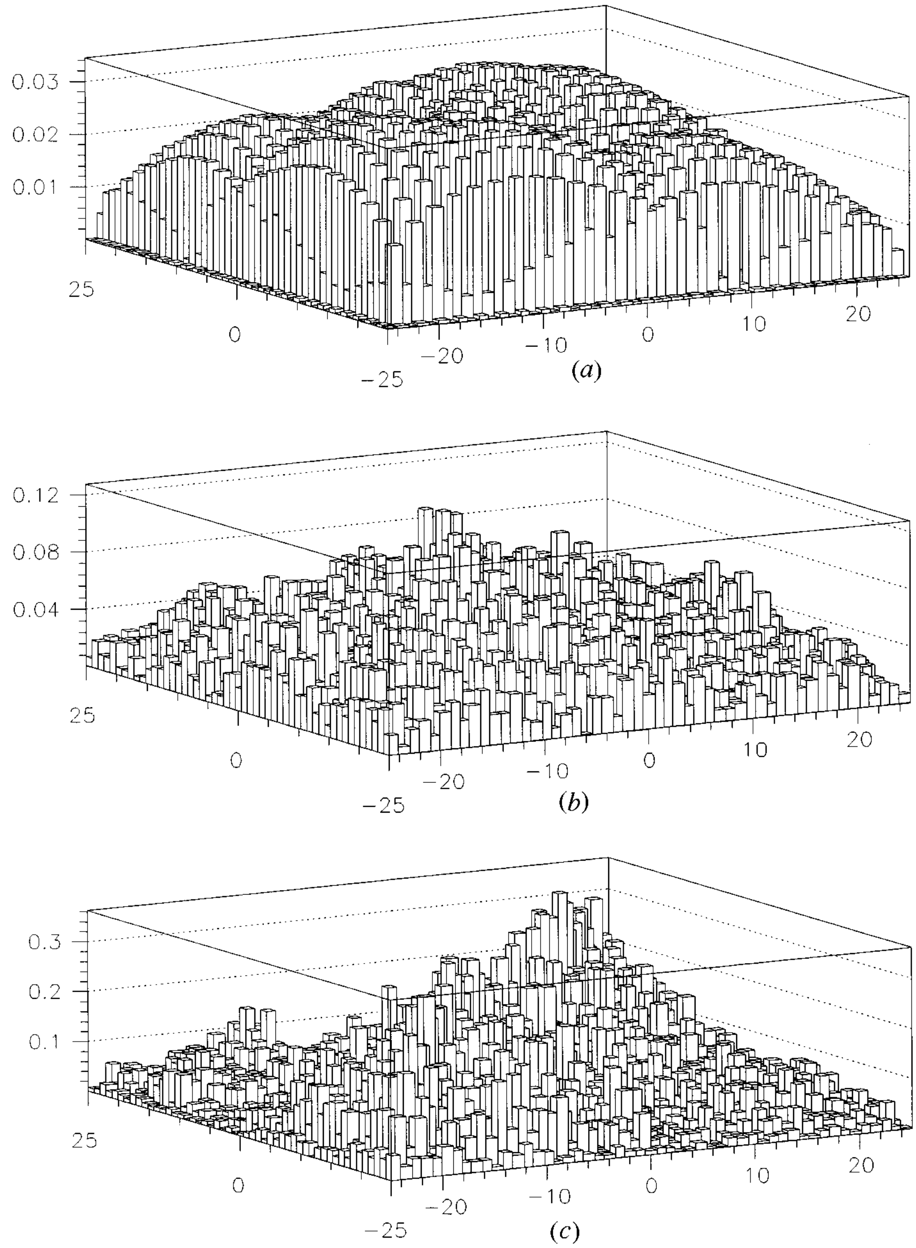

Fig. 7. The moduli of the T-matrix.

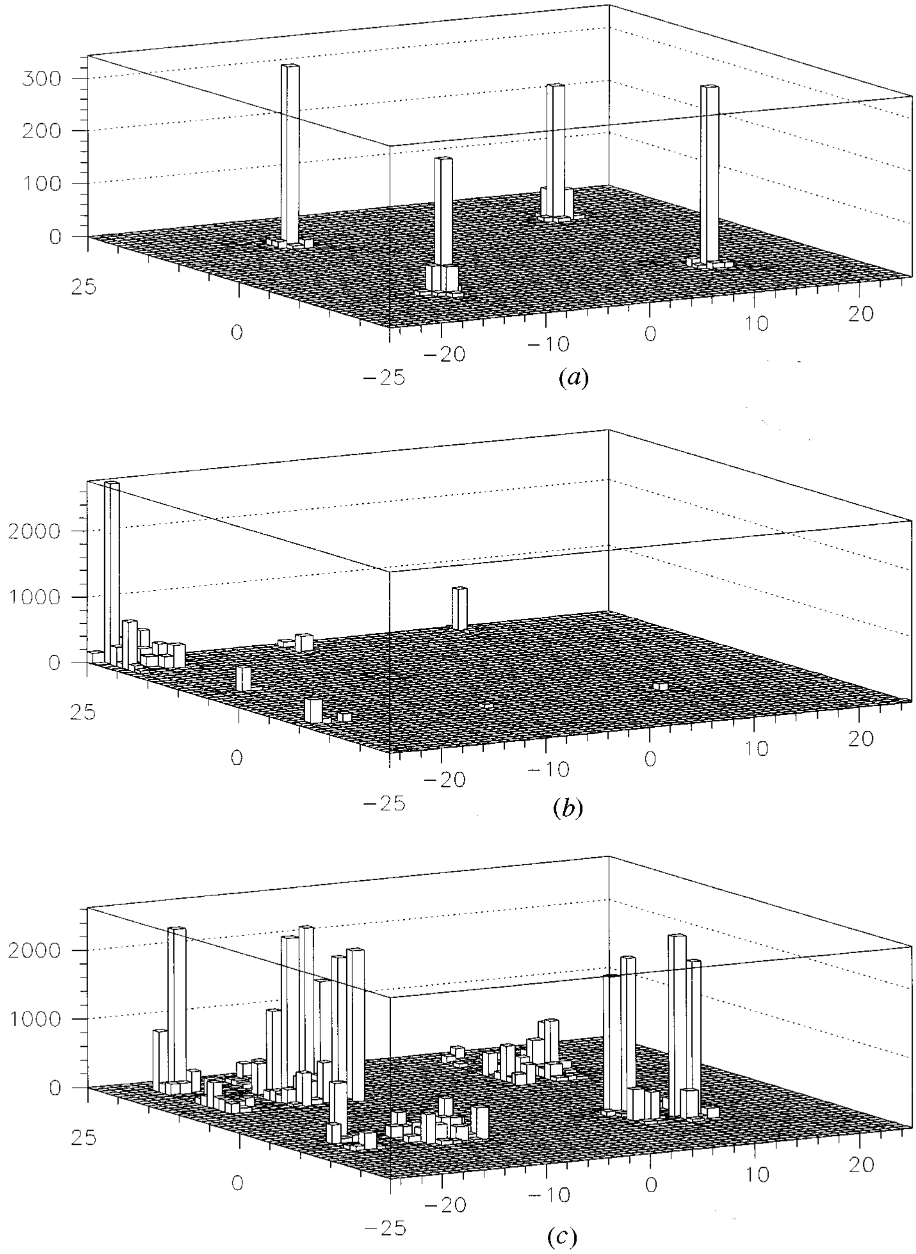

Fig. 8. The 2D Fourier transformation of the T-matrix moduli.

The enhancement of the repulsion parameter γ in Figs 6*c* and 6*d* clearly demonstrates the development of the 'chaos' of the S-matrix when the number of harmonics increases. To explain this behaviour let us consider the structure of the S-matrix (see equation 21). It consists of the product of three matrices. The distribution of level spacing for each one is regular but their product can possess random properties. The degree of this randomness depends on the internal structure of the middle $\hat{S}^{\rm res}$ part.

Fig. 7 represents the moduli of the $\hat{T}^{\rm res}$-matrix for (*a*) one, (*b*) two and (*c*) many harmonic (C 'asymmetric rectangle') modulation functions, while Fig. 8 gives a power spectrum of the two-dimensional Fourier transformation of each of these T-matrices. The growth in complexity of the T-matrix from Fig. 7*a* to 7*c* is evident, especially so in Fig. 8. This situation, in a sense, is similar to the quantum kick-rotator model (Izrailev 1990), where the unitary evolution operator $\hat{U}$ has an identical structure.

4. Discussion and Conclusions

In the present work we have investigated a model without an explicit classical analogue for which quantum effects play an important role. The important observation is that quantum chaos can exist only in the restricted range of the energies where the ratio $\bar{\Gamma}/\bar{D}$ is close to unity.

We have found that our model with a periodic modulation function demonstrates only a transition to weak chaos and some statistical properties of the S-matrix essentially deviate from RMT predictions. However, the chaotic properties of the S-matrix become stronger as the complexity of the modulation function is increased. A point that should be mentioned is that computing resources confine our treatment of many-harmonic potentials to values of $\alpha \approx 2 \times 10^{-4}$ and one might expect even stronger random behaviour of the S-matrix at smaller permeabilities.

Another question which requires further investigation is the increase in the complexity of the potential when $g(y)$ goes towards a quasi-periodic form; for example, $g(y) = g_1(\nu r y) + g_2(\nu s y)$, where $r, s \to \infty$ and are mutually primes. So far, we have investigated only small r and s, up to $r = 5$ and $s = 8$. We found that the degree of chaos is not stronger than the corresponding 'periodic' $(r, s = 1)$ potential for the accessible range of parameters α and k.

Acknowledgments

I am very thankful to V. V. Sokolov, who suggested studying this model, and to F. M. Izrailev for instructive and useful discussions.

References

Bleher, S., Ott, E., and Grebodi, C. (1989). *Phys. Rev. Lett.* **63**, 919.
Blümel, R., and Smilansky, U. (1989). *Physica* D **36**, 111.
Blümel, R., Dietz, B., Jung, C., and Smilansky, U. (1992). *J. Phys.* A **25**, 1483.
Csordás, A., and Šeba, P. (1993). *Chaos* **3**, 637.
Ericson, T. (1963). *Ann. Phys. (New York)* **23**, 390.
Gaspard, P., and Rice, S. A. J. (1989). *Chem. Phys.* **90**, 2242.
Izrailev, F. M. (1990). *Phys. Rep.* **196**, 299.
Jones, W. B., and Tron, W. J. (1980). 'Continued Fractions' (Addison-Wesley: Reading).
Jung, C. (1986). *J. Phys.* A **19**, 1345.

Landau, L. D., and Lifshitz, M. E. (1965). 'Quantum Mechanics' (Pergamon: New York).
Manakov, S. V., and Shchur, L. N. (1983). *Sov. Phys. JETP* **37**, 54.
Mehta, M. L. (1990). 'Random Matrices', 2nd edn (Academic: New York).
Morse, P. M., and Feshbach, H. (1953). 'Methods of Theoretical Physics' (McGraw–Hill: New York).
Pereyra, P., and Mello, P. A. (1983). *J. Phys.* A **16**, 237.
Porter, C. E. (1965). 'Statistical Theory of Spectra: Fluctuations' (Academic: New York).
Smilansky, U. (1992). Proc. 1989 Les Houches Summer School on Chaos and Quantum Physics (Eds M.-J. Giannoni *et al.*), p. 341 (North Holland: Amsterdam).

Appendix A: Solving a System of Linear Equations represented by an Infinite Tridiagonal Matrix

Our system can be represented in matrix form as

$$\hat{\mathbf{A}}\,\vec{\varphi}_{\mathrm{l}} = \vec{\mathbf{I}}_{\mathrm{l}}\ , \tag{A1}$$

where

$$\hat{\mathbf{A}} = \begin{pmatrix} \ddots & \ddots & \ddots & \ddots & \ddots \\ \ddots & a_{-1} & \beta & O & \ddots \\ \ddots & \beta & a_0 & \beta & \ddots \\ \ddots & O & \beta & a_1 & \ddots \\ \ddots & \ddots & \ddots & \ddots & \ddots \end{pmatrix}\ ,\ \vec{\varphi}_{\mathrm{l}} = \begin{pmatrix} \vdots \\ \varphi_{-1l} \\ \varphi_{0l} \\ \vdots \\ \varphi_{ll} \\ \vdots \end{pmatrix}\ ,\ \vec{\mathbf{I}}_{\mathrm{l}} = \begin{pmatrix} \vdots \\ 0 \\ 0 \\ \vdots \\ \lambda_l \\ \vdots \end{pmatrix} = \lambda_l\,\delta_{ml}\,. \tag{A2}$$

As a matter of convenience let us introduce the following notation for half-infinite determinants:

$$D_m^{\infty} = \begin{vmatrix} a_m & \beta & 0 & \dots \\ \beta & a_{m+1} & \beta & \dots \\ 0 & \beta & a_{m+2} & \dots \\ \vdots & \vdots & \vdots & \ddots \end{vmatrix}\ ,\ D_m^{-\infty} = \begin{vmatrix} \ddots & \vdots & \vdots & \vdots \\ \dots & a_{m-2} & \beta & 0 \\ \dots & \beta & a_{m-1} & \beta \\ \dots & 0 & \beta & a_m \end{vmatrix}\,. \tag{A3}$$

It is simple to see that

$$D_m^{\infty} = a_m D_{m+1}^{\infty} - \beta^2 D_{m+2}^{\infty}, \qquad D_m^{-\infty} = a_m D_{m-1}^{-\infty} - \beta^2 D_{m-2}^{-\infty}\,. \tag{A4}$$

We may express $\det(\hat{\mathbf{A}})$ through $D_m^{\pm\infty}$ after decomposing it along the mth row:

$$\det(\hat{\mathbf{A}}) \equiv D_{-\infty}^{\infty} \ = \ a_m D_{m-1}^{-\infty} D_{m+1}^{\infty} - \beta^2\left(D_{m-2}^{-\infty} D_{m+1}^{\infty} + D_{m-1}^{-\infty} D_{m+2}^{\infty}\right)\,. \tag{A5}$$

According to Crammer's rule the solution of (A1) is

$$\varphi_{nl} \ = \ \lambda_l \hat{\mathbf{A}}_{nl}^{-1} = \frac{\det(\hat{\mathbf{A}}'_n)}{\det(\hat{\mathbf{A}})}\ , \tag{A6}$$

where $\det(\hat{\mathbf{A}}'_n)$ is obtained from $\det(\hat{\mathbf{A}})$ by replacing the nth column with $\vec{\mathbf{I}}_{\mathbf{l}}$.

We now express $\det(\hat{\mathbf{A}}'_n)$ in terms of the notation of (A3). Consider the case of $n < l$; then

$$\det(\hat{\mathbf{A}}'_n) = \begin{vmatrix} \cdots & \cdots & \cdots & \cdots & \cdots & \cdots & \cdots & \cdots & \cdots & \cdots \\ \vdots & a_{n-2} & \beta & 0 & & & & & & \vdots \\ \vdots & & \beta & 0 & \beta & & & 0 & & \vdots \\ \vdots & & & 0 & a_{n+1} & \beta & & & & \vdots \\ \vdots & & & 0 & \beta & a_{n+2} & \beta & & & \vdots \\ \vdots & & & \vdots & \ddots & \ddots & \ddots & & & \vdots \\ \vdots & 0 & & 0 & & \beta & a_{l-1} & \beta & & \vdots \\ \vdots & & & \lambda_l & & & \beta & a_l & \beta & \vdots \\ \vdots & & & 0 & & & & \beta & a_{l+1} & \vdots \\ \cdots & \cdots & \cdots & \cdots & \cdots & \cdots & \cdots & \cdots & \cdots & \cdots \end{vmatrix}$$

$$= (-1)^{n+l}\lambda_l \begin{vmatrix} \cdots & \cdots & \cdots & \cdots & \cdots & \cdots & \cdots & \cdots & \cdots & \cdots \\ \vdots & a_{n-2} & \beta & & & & & & & \vdots \\ \vdots & \beta & a_{n-1} & & & & & & & \vdots \\ \vdots & & \beta & \beta & & & & & & \vdots \\ \vdots & & & a_{n+1} & \beta & & & 0 & & \vdots \\ \vdots & & & \beta & a_{n+2} & \beta & & & & \vdots \\ \vdots & & \vdots & \ddots & \ddots & \ddots & & \vdots & & \vdots \\ \vdots & 0 & & & \beta & a_{l-1} & \beta & & & \vdots \\ \vdots & & & & & & \beta & a_{l+1} & \beta & \vdots \\ \vdots & & & & & & & \beta & a_{l+2} & \vdots \\ \cdots & \cdots & \cdots & \cdots & \cdots & \cdots & \cdots & \cdots & \cdots & \cdots \end{vmatrix} . \tag{A7}$$

The determinant (A7) is equal to the product of the determinants of the three blocks, according to the theorem about a cellular matrix's determinant. The central block is lower-triangular and the other blocks are tridiagonal. Thus we get

$$\det(\hat{\mathbf{A}}'_n) = (-1)^{n+l}\lambda_l D_{n-1}^{-\infty}\beta^{l-n} D_{l+1}^{\infty} . \tag{A8}$$

The case $n > l$ is done in a similar manner and the common solution of (A6) can be written as

$$\varphi_{nl} = \frac{(-1)^{n+l}\lambda_l\beta^{|n-l|}}{\det(\hat{\mathbf{A}})} \times \begin{cases} D_{n-1}^{-\infty}D_{l+1}^{\infty}, & n \le l \\ D_{l-1}^{-\infty}D_{n+1}^{\infty}, & n \ge l \end{cases} \tag{A9}$$

In particular, the diagonal element φ_{ll} [after application of (A5) to $\det(\hat{\mathbf{A}})$ in terms of the lth row] is

$$\varphi_{ll} \;=\; \frac{\lambda_l}{a_l - \beta^2 \left[\dfrac{D^{-\infty}_{l-2}}{D^{-\infty}_{l-1}} + \dfrac{D^{\infty}_{l+2}}{D^{\infty}_{l+1}} \right]} \;\equiv \frac{\lambda_l}{a_l - \beta \left[f^{(-)}_{l-1} + f^{(+)}_{l+1} \right]} . \tag{A10}$$

Here we introduced the symbols:

$$f^{(-)}_n = \beta \frac{D^{-\infty}_{n-1}}{D^{-\infty}_n}, \quad f^{(+)}_n = \beta \frac{D^{\infty}_{n+1}}{D^{\infty}_n} . \tag{A11}$$

The coefficients φ_{nl} may be written using φ_{ll} and the notation in (A11). For example, we have for the case $n < l$

$$\varphi_{nl} = (-1)^{l-n} \beta^{l-n} \varphi_{ll} \frac{D^{-\infty}_{n-1}}{D^{-\infty}_{l-1}} ,$$

but

$$\beta^{l-n} \frac{D^{-\infty}_{n-1}}{D^{-\infty}_{l-1}} = \beta^{l-n} \frac{D^{-\infty}_{n-1}}{D^{-\infty}_{n}} \frac{D^{-\infty}_{n}}{D^{-\infty}_{n+1}} \cdots \frac{D^{-\infty}_{l}}{D^{-\infty}_{l-1}} = \prod_{j=n}^{l-1} f^{(-)}_j . \tag{A12}$$

Hence, the general solution is

$$\varphi_{\,ll} = \frac{\lambda_l}{a_l - \beta \left[f^{(-)}_{l-1} + f^{(+)}_{l+1} \right]},$$

$$\varphi_{nl} = (-1)^{|l-n|} \varphi_{ll} \times \begin{cases} \Pi_{j=n}^{l-1} f^{(-)}_j, & n < l \\ \Pi_{j=l+1}^{n} f^{(+)}_j, & n > l \end{cases} . \tag{A13}$$

From equation (A4) it follows that the $f^{(\pm)}_n$ are continued fractions:

$$f^{(\pm)}_n = \frac{1}{\frac{a_n}{\beta} - \frac{1}{a_n \pm 1} \beta \cdots} = \frac{1}{\frac{a_n}{b} - {}^{(\pm)}_{n\pm1}} . \tag{A14}$$

Thus if we are only interested in a finite number of elements, φ_{nl}, with $-L_{\min} \leq n, l \leq L_{\max}$, we only need to calculate two continued fractions $f^{(-)}_{-L_{\min}}$ and $f^{(+)}_{L_{\max}}$! After that we can find all the required elements with the help of (A13) and (A14).

It is worth noting that if $a_n = 1$ and $\beta < \frac{1}{2}$, then

$$\hat{\mathbf{A}}^{-1}_{nl} = \frac{(-1)^{n+l}}{\sqrt{1 - 4\beta^2}} \left[\frac{2\beta}{1 + \sqrt{1 - 4\beta^2}} \right]^{|n-l|} . \tag{A15}$$

Appendix B: Calculation of Continued Fraction's Remainder

Consider $n > L \equiv \max(L_{\max}, L_{\min}) > 0$, where $L_{\max}$ and $L_{\min}$ are determined by equation (15). For such n, the y-component of $\vec{k}$ has $|k_{y_n}| > k$ and consequently

$$k_{x_n} = \sqrt{k^2 - k_{y_n}^2} = i|k_{x_n}|\,. \tag{B1}$$

But this means that the elements (32) of the continued fraction (31) are real:

$$a_n = \frac{\beta_0\left(1 - e^{-2|k_{x_n}|d}\right) + \alpha|k_{x_n}|}{1 - e^{-2|k_{x_n}|d}}\,. \tag{B2}$$

For the sake of convenience we work with dimensionless values:

$$\tilde{\alpha} = \alpha\nu; \qquad \vec{q} = \frac{q}{\nu} \quad , \; -\frac{1}{2} \leq \vec{q} \leq \frac{1}{2}; \qquad \vec{k} = \frac{k}{\nu}.$$

Therefore, we get

$$|\tilde{k}_{x_n}| = (n + \tilde{q})\sqrt{1 - \left(\frac{\tilde{k}}{n + \tilde{q}}\right)^2}\,, \tag{B4}$$

where

$$n + \tilde{q} > \tilde{k} > 0\,. \tag{B5}$$

It is clear that in the limit $n \to \infty$, a_n has no dependence on k and the remainder of the continued fraction may be written as follows:

$$f_{\pm n}^{(\pm)} = \frac{1}{\frac{\beta_0 + \tilde{\alpha}(n \pm \tilde{q})}{\beta} - \frac{1}{\frac{\beta_0 + \tilde{\alpha}(n+1 \pm q)}{\beta} - \cdots}}\,. \tag{B6}$$

On the other hand, by using the recurrence formula for Bessel functions

$$\mathbf{J}_{x-1}(z) = \frac{2x}{z}\mathbf{J}_x(z) + \mathbf{J}_{x+1}(z),$$

we find that

$$\frac{\mathbf{J}_{x+n}(z)}{\mathbf{J}_{x+n-1}(z)} = \frac{1}{\frac{2(x+n)}{z} - 1/\frac{2(x+n+1)-\cdots}{z}}\,. \tag{B7}$$

And comparing (B7) with (B6) we obtain

$$f_{\pm \mathrm{n}}^{(\pm)} = \frac{\mathbf{J}_{\beta_0/\tilde{\alpha}\pm\tilde{q}+n}(2\beta/\hat{\alpha})}{\mathbf{J}_{\beta_0/\tilde{\alpha}\pm\tilde{q}+n-1}(2\beta/\hat{\alpha})}, \quad n \gg \tilde{k}\,. \tag{B8}$$

In numerical calculations it is necessary to know where the fraction (B6) will begin to converge and where it may be cut off to give a solution with a given accuracy. The following theorem (see Jones and Tron 1980) gives the answer:

Theorem 1 *The continued fraction (A14) will converge if*

$$|a_n/\beta| > 2\,. \tag{B9}$$

From (B9) and (B5) it follows that convergent behaviour occurs for values of n that satisfy the condition

$$n > \max\left(\frac{2\beta - \beta_0}{\alpha\nu}, \tilde{k}\right)\,. \tag{B10}$$

Appendix C: Solution of the Integral Equation for φ

If a modulation function has a lot of harmonics [for example when $g(y)$ constructed of a set of rectangular pulses], it is more convenient to numerically solve the integral equation for the function $\varphi(y)$ in coordinate space instead of the system (17). For these purposes let us rewrite (10), by using (11) and (13), in the following form:

$$\varphi(y) = e^{il\nu y}\left(1 - e^{ik_{xl}2d}\right) - \frac{i}{2}\int_{-\pi/\nu}^{\pi/\nu} G_{\mathrm{lat}}(k,q,d;t)g(t+y)e^{iqt}\varphi(t+y)dt\,. \tag{C1}$$

Here the lattice Green's function is defined as

$$G_{\mathrm{lat}}(k,q,d;t) = \sum_{n=-\infty}^{\infty} e^{iq/\nu 2\pi t}\Big[H_0^{(1)}\left(k|t+2\pi/\nu n|\right) - H_0^{(1)}\left(k\sqrt{4d^2+(t+2\pi/\nu n)^2}\right)\Big]. \tag{C2}$$

With Poisson's formula

$$\sum_{n=-\infty}^{\infty} f(2\pi n) = \frac{1}{2\pi}\sum_{l=-\infty}^{\infty} F(l), \qquad F(x) = \int_{-\infty}^{\infty} e^{ix\tau}f(\tau)d\tau$$

and the familiar integral representation of Hankel's function,

$$H_0^{(1)}(k\sqrt{a^2+t^2}) = -\frac{i}{\pi^2}\int_{-\infty}^{\infty} e^{ih_x a}dh_x \int_{-\infty}^{\infty}\frac{e^{ih_y t}dh_y}{h_x^2+h_y^2-k^2}$$

the sum (C2) can be simplified (Morse and Feshbach 1953):

$$G_{lat}(k,q,d;t) = \frac{e^{-iqt}}{\pi} \sum_{l=-\infty}^{\infty} e^{-il\nu t} \frac{1 - e^{2ik_{xl}d}}{k_{xl}} \,. \tag{C3}$$

A numerical investigation of (C1) shows that the series (C3) can be truncated, starting from any

$$|L| \geq \frac{1}{|\alpha|\nu} \,, \tag{C4}$$

where α is the permeability. The condition (C4) can be interpreted physically as follows: when a ‘particle’ is in a periodic potential with a depth of order $1/\alpha$, it excites $L \sim 1/\alpha\nu$ harmonics.

Manuscript received 13 November 1998, accepted 1 June 1999